Research Article

For reprint orders, please contact: reprints@futuremedicine.com

Nanomedicine

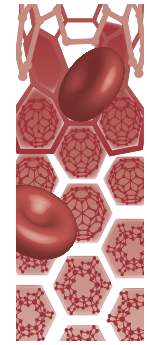

A strategy for combating melanoma with oncogenic c-Myc inhibitors and targeted nanotherapy

Aims: The activity of the transcription factor *c-Myc* is dependent upon heterodimerization with Max to control target gene transcription. Small-molecule inhibitors of c-Myc–Max have exhibited low potency and poor water solubility and are therefore unsuitable for *in vivo* application. We hypothesized that a nanomedicine approach incorporating a cryptic c-Myc inhibitor prodrug could be delivered and enzymatically released in order to effectively inhibit melanoma. **Materials & methods:** An Sn-2 lipase-labile Myc inhibitor prodrug was synthesized and included in two $\alpha_v\beta_3$-targeted nanoparticle platforms (20 and 200 nm). The inherent antiproliferate potency was compared with the lipid-free compound using human and mouse melanoma cell lines. **Results & conclusion:** These data demonstrate for the first time a successful nanodelivery of c-Myc inhibitors and their potential use to prevent melanoma.

Keywords: c-Myc inhibitor • melanoma • nanotherapy • prodrug

Dipanjan Pan*[1,2], Benjamin Kim[1], Grace Hu[1], Deepti Sood Gupta[1], Angana Senpan[1], Xiaoxia Yang[1], Anne Schmieder[1], Corban Swain[1], Samuel A Wickline[1], Michael H Tomasson[1] & Gregory M Lanza[1]

[1]Department of Medicine, Washington University School of Medicine, 4320 Forest Park Avenue, Saint Louis, MO 63108, USA

[2]Department of Bioengineering, University of Illinois at Urbana-Champaign, Biomedical Research Center, Office 3304, 3rd Floor, Mills Breast Cancer Institute & Carle Foundation Hospital, 502 N. Busey, Urbana, IL 61801, USA

*Author for correspondence:
Tel.: +1 217 244 2938
dipanjan@illinois.edu

The *c-Myc* gene is a transcription factor that is speculated to regulate the expression of 15% of all genes and is involved in one out of seven cancer-related casualties [1–6]. *c-Myc* activity is dependent upon heterodimerization cofactors, such as with Max, to control target gene transcription [7–14]. Small-molecule inhibitors of c-Myc–Max have been explored as potential therapeutic agents [4–16]. Most of them have exhibited low potency and were often hydrophobic, making them pharmaceutically difficult to formulate and practically deliver for clinical translation.

Very recently, using lipid-encapsulated perfluorocarbon (PFC) nanoparticles (NP), we have reported the concept of contact-facilitated drug delivery, which refers to the process by which the bound NP lipid surfactant components transfer to the targeted cell through a hemifusion complexation of the NP with target cell lipid membranes [17,18]. In effect, this approach delivers a 'kiss of death' without the requisite cellular internalization of the NPs and escape of the drug payload from an endosomal compartment. These NPs are vascularly constrained (>150 nm) and have been homed to a myriad of biological markers for application in diagnostic imaging and ligand-directed drug delivery for cancer, atherosclerosis, restenosis and rheumatoid arthritis [4–7]. However, *in vivo* pharmacokinetic studies tracking NP membrane-dissolved drugs revealed that even very hydrophobic compounds were partially released *in vivo* prematurely [18].

We hypothesize that a targeted phospholipid NP approach against melanoma with the surfactant inclusion of a c-Myc inhibitor in the form of an Sn-2 phospholipid prodrug (PD) would ultimately improve potency, prevent early intravascular loss and mitigate against off-target toxicity. Towards this aim, we intend to develop an Sn-2 c-Myc-PD, stably incorporate the compound into integrin-targeted PFC NPs and effectively inhibit the proliferation of melanoma cells in culture with improved potency versus the free drug. We also hypothesize that specific targeting can be achieved irrespective of the intra- or extra-vascular property of the NPs

Future Medicine part of fsg

(20–200 nm). The objectives of the present work were: to develop and characterize an Sn-2 lipase-labile PD of a c-Myc inhibitor; to demonstrate the stability of the c-Myc-PD in the PFC NPs; to demonstrate the therapeutic efficacy of the agent *in vitro* in mouse and human melanoma cells; and to investigate the preliminary *in vivo* properties of these agents through biodistribution and pharmacokinetic studies.

Towards this goal, we developed phospholipid-encapsulated, mixed-micellar NPs (~20 nm, polysorbate cored). A simple and straightforward procedure was followed to introduce the PD to the NPs. The PD was incorporated within the phospholipid–surfactant mixture as a nominal 2 mol%. A higher (10 mol%) loading was successfully achieved for the PFC NP system. However, our attempts to prepare the smaller particles with such high loading failed, resulting in particle aggregation (>700 nm). We demonstrated that both intravascular (~200 nm) and extravascular (~20 nm) c-Myc NPs markedly decreased human and mouse cell proliferation more effectively than the free drug at equimolar concentrations.

Materials & methods

Unless otherwise listed, all solvents and reagents were purchased from Aldrich Chemical Co. (MO, USA) and used as received. Anhydrous chloroform and methanol were purchased from Aldrich Chemical Co. Perfluorooctylbromide was purchased and used as received from Exfluor, Inc. (TX, USA). High-purity egg yolk phosphatidylcholine was purchased from Avanti Polar Lipids, Inc (AL, USA). Argon and nitrogen (ultra-high purity: 99.99%) were used for the storage of materials. The Spectra/Por® membrane (cellulose molecular weight cut-off [MWCO]: 20,000 Da) used for dialysis was obtained from Spectrum Medical Industries, Inc. (CA, USA).

Typical procedure for the preparation of $\alpha_v\beta_3$-targeted c-Myc & control NPs

Phospholipid-encapsulated PFC NPs were prepared as microfluidized suspensions of 20% (v/v) 15:5 perfluorocrown ether (Exfluor, Inc.), 2.0% (w/v) of a surfactant comixture and 1.7% (w/v) glycerin in pH 6.5 carbonate buffer (Figure 1A). An $\alpha_v\beta_3$-integrin antagonist, a quinalone nonpeptide developed by Bristol-Myers Squibb Medical Imaging (MA, USA; US patent 6511648 and related patents), was used for homing angiogenesis. The surfactant co-mixture of NPs included approximately 96.5 mol% lecithin, 0.15 mol% of $\alpha_v\beta_3$-ligand-conjugated lipid and 2 mol% of c-Myc-PD. Nontargeted NPs excluded the homing ligands. The surfactant components for each formulation were combined with the PFC, buffer and glycerin with pH adjusted to 6.5, and the mixtures were homogenized at 20,000 psi for 4 min. The NPs were preserved under inert gas in sterile sealed vials until use. For *in vitro* evaluation, three NP formulations were prepared: $\alpha_v\beta_3$-targeted c-Myc-PD PFC NPs ($\alpha_v\beta_3$-c-Myc-PD PFC NPs); $\alpha_v\beta_3$-targeted no drug PFC NPs ($\alpha_v\beta_3$-ND NPs); and nontargeted c-Myc-PD PFC NPs (NT-c-Myc-PD PFC NPs).

The $\alpha_v\beta_3$-integrin antagonist was initially reported as the ^{111}In-DOTA conjugate RP748 and cyan 5.5 homolog TA145 [18]. The $\alpha_v\beta_3$-ligand has a 15-fold preference for the Mn^{2+}-activated receptor (21 nmol/l) and an IC_{50} for $\alpha_v\beta_5$, $\alpha_5\beta_1$ and Gp-IIbIIIa of >10 μM [Bristol-Myers Squibb Medical Imaging, Unpublished data] [18–21]. The NPs have an IC_{50} of 50 pM for the Mn^{2+}-activated $\alpha_v\beta_3$-integrin [Kereos, Inc., Unpublished data].

D_{av}/DLS: 210 ± 32 nm; ζ-potential: -25 ± 6 mV; PDI: ~0.14; D_{ah}/TEM: 172 ± 66 nm. D_{av} refers to number-averaged hydrodynamic diameter from dynamic light scattering measurements in hydrated state with electrophoretic mobility or ζ-potential as -25 ± 6 mV and polydispersity index (PDI) as ~0.14; D_{ah} is anhydrous state diameter obtained from transmission electron microscope (TEM).

In vitro dissolution of c-Myc-PD from NPs

In vitro dissolution revealed that the PD was well retained with less than 9% of the incorporated dosage diffusing from the NPs under infinite sink conditions during *in vitro* dissolution. The release of the drug was monitored by ultraviolet (UV)–visible spectroscopy. The majority of drug release occurred during the first day (6%), with further losses undetectable between days 2 and 4. Spectra for dialysis tubing (biotechnology-grade membranes [regenerated cellulose] MWCO = 50,000; 8 × 5 mm; 0.25 ml/cm; 15 m; lot #27007) was from Spectrum Laboratories, Inc. (CA, USA). Spin-x® microcentrifuge tube filters (0.22 μm cellulose acetate in 2.0 ml polypropylene tubes; 25/pack; 100/case; nonsterile) were from Corning, Inc. (NY, USA). NaCl was from Sigma (MO, USA). Human serum albumin was from Sigma and was fatty acid free and globulin free. NaN_3 sodium azide was from Sigma. 4 ml amber autosampler vials with polytetrafluoroethylene (PTFE) septa were from National Scientific Co. (TN, USA) cat# c4015-21W. Presterilized 500-ml vacuum-driven disposable filtration system (0.22 μm; GP Express® PLUS Membrane) was from Millipore Corp. (MA, USA). Acrodisc® syringe filters (0.2 μm super® Membrane; nonpyrogenic; ref.: 4612) were from the Pall Gelman laboratory (NY, USA). Free c-Myc was analyzed by an UV absorbance spectrometer at wavelength 280–320 nm for detection.

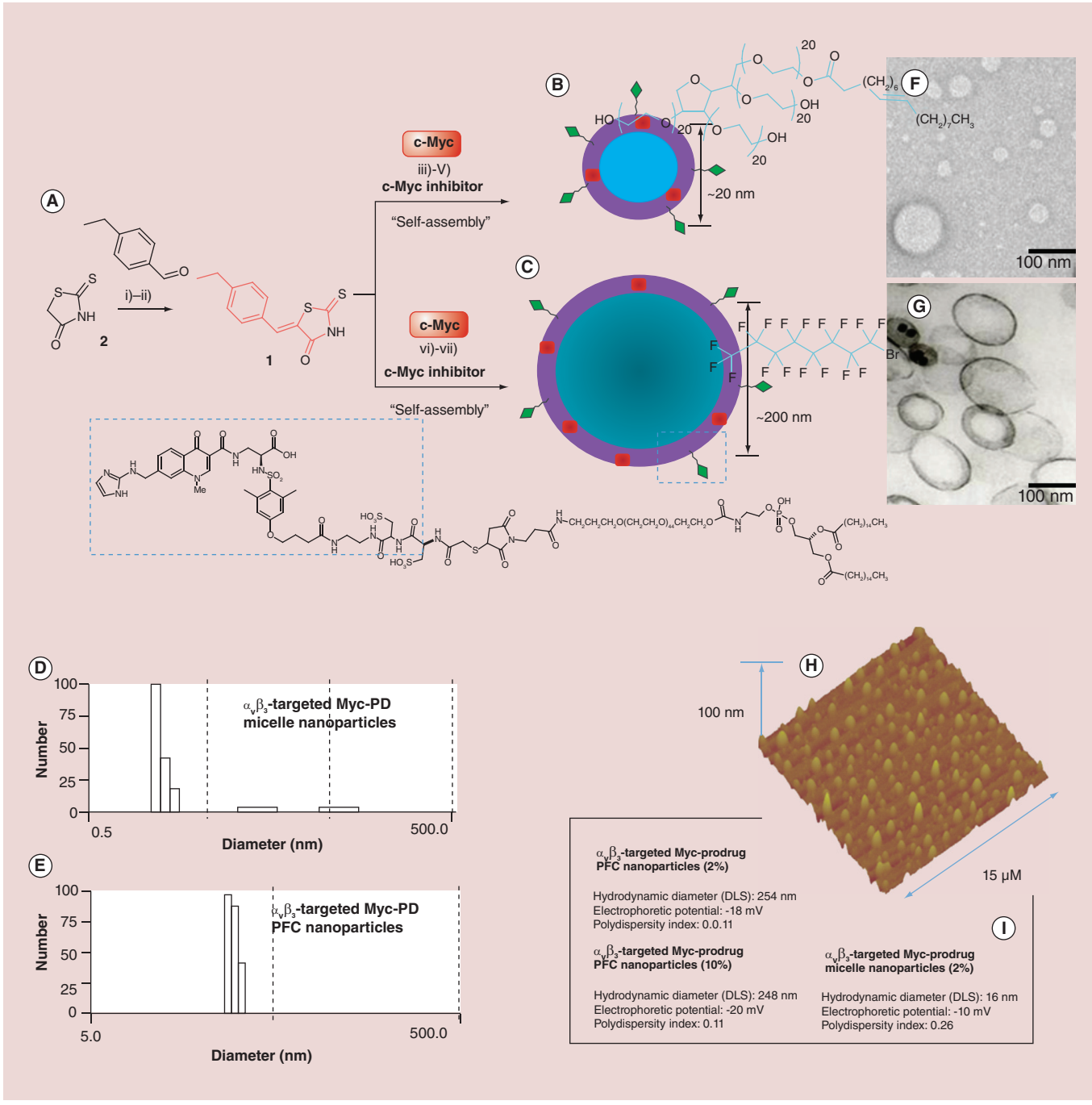

Figure 1. Synthesis and characterization of nanoparticles. (A) Synthesis of c-Myc-PD: **(i & ii)** aldol condensation of 4-ethyl benzaldehyde and rhodanine/Tween® 80/K_2CO_3; **(iii)** piperidine-mono-*tert*-boc (N-tert-butoxycarbonyl), formaldehyde; deprotection of tert-Boc: HCl/dioxane; **(iv)** PAzPC/DMAP/DCC, RT 24 h; **(v)** preparation of lipid thin film from a phospholipid mixture of 97.6 mol% lecithin PC, 0.15 mol% of $\alpha_v\beta_3$-ligand-conjugated lipid and 2 mol% of c-Myc-PD; self-assembly by brief sonication and microfluidization, **(B)** sorbitan sesquioleate or **(C)** perfluorocarbon and glycerin, pH 6.5, at 20,000 psi for 4 min. Physicochemical characterization of $\alpha_v\beta_3$-targeted c-Myc nanoparticles: **(D & E)** number-averaged hydrodynamic dynamic light scattering particle size distribution of targeted c-Myc nanoparticles; **(F & G)** transmission electron micrograph images of c-Myc-PD nanoparticles; **(H)** AFM image of the polysorbate micelles; **(I)** characterization table.
AFM: Atomic force microscopy; DCC:N,N′-Dicyclohexylcarbodiimide; DMAP:4-Dimethylaminopyridine; PAzPC: 1-palmitoyl-2-azelaoyl-sn-glycero-3-phosphocholine; PD: Prodrug; PFC: Perfluorocarbon; RT: Room temperature.

Procedure

A total of 1 mg/ml of ethanol-free c-Myc (10058-F4) solution was diluted to 100 or 10 µg/ml solutions with $CHCl_3$:ethanol (1:1) and the UV absorbance was measured measure at 300 nm to generate a calibration standard. Dialysis tubing was cut to approximately 8-cm lengths and soaked in 2 l deionized (DI) water for at least 30 min. It was then rinsed well with DI water and a knot was tied at one end. Saline was used as a releasing medium (0.9% NaCl). A pipette was used to add 0.25 ml c-Myc NPs to each of three dialysis tubings. The end was tied and rinsed with DI water before being placed in an autosampler vial filled with 3.5 ml of releasing medium. The cap was parafilmed to incubate samples in a rocker at 37°C. The samples were transferred to 3.5 ml of fresh releasing medium each day and UV absorbance was measured at 300 nm. At 0 day-1/2, 125 µl of c-Myc NPs was mixed with 375 µl of Cleanascite™ (HC product #LGC1050; lot #103061; from CPG, Inc., WI, USA) and incubated for approximately 30 min at room temperature (RT) then centrifuged for 10 min at 5000 rpm. A total of 250 µl of supernatant was taken and dissolved into 0.75 ml of saline, then the UV absorbance was recorded.

c-Myc-PD *in vitro* cell viability assay

Human (C32) and mouse (B16-F10) melanoma cell lines were seeded at 2500 cells/well in a 96-well plate. After 24 h, the cells were treated with $\alpha_v\beta_3$-Myc-PD NPs, $\alpha_v\beta_3$-ND NPs, NT-c-Myc-PD NPs, free c-Myc-PD, DMSO or complete media for 2 h (eight replicates per sample per plate). Wells were washed three times with phosphate-buffered saline post-treatment and plates were returned to the incubator. From 1, 2 and 3 days after drug exposure, the following assays were used to test the effects on cell metabolism and proliferation: cell metabolic activity was measured using AlamarBlue® (Invitrogen, CA, USA), which is based on the reduction of a nonfluorescent dye to a fluorescent substrate in metabolically active cells. This reduction is typically attributed to different oxidoreductase enzyme systems that use NAD(P)H as the primary electron donor. The redox reaction was monitored using a fluorescence plate reader (excitation [E_x] = 570 nm, emission [E_m] = 585 nm) in which the resulting signal is proportional to the number of viable cells present. The signal intensity from each sample was normalized to a blank sample (no cells with complete media) and four plates were assessed per time point.

Dynamic light scattering measurements

Hydrodynamic diameter distributions and distribution averages for the c-Myc-PD PFC NPs and controls in aqueous solutions were determined by dynamic light scattering. Hydrodynamic diameters were determined using a Brookhaven Instrument Co. (NY, USA) ZetaPlus® particle size analyzer. Measurements were made following dialysis (MWCO 10-kDa dialysis tubing; Spectrum Laboratories, Inc.) of PFC NP suspensions into DI water (0.2 mM). NPs were dialyzed into water prior to analysis. Scattered light was collected at a fixed angle of 90°. A photomultiplier aperture of 400 mm was used, and the incident laser power was adjusted in order to obtain a photon counting rate of between 200 and 300 kcps. Only measurements for which the measured and calculated baselines of the intensity autocorrelation function agreed to within +0.1% were used for calculating the NP hydrodynamic diameter values. All determinations were made in multiples of five consecutive measurements.

Electrophoretic potential measurements

ζ-potential values for the c-Myc-PD PFC NPs were determined with a ZetaPlus ζ-potential analyzer. Measurements were made following dialysis (MWCO 10-kDa dialysis tubing; Spectrum Laboratories) of PFC NP suspensions into water. Data were acquired in the phase analysis light scattering mode following solution equilibration at 25°C. Calculation of the ζ-potential from the measured NP electrophoretic mobility (µ) employed the Smoluchowski equation: $\mu = \varepsilon\zeta\eta$, where ε and η are the dielectric constant and the absolute viscosity of the medium, respectively. Measurements of the ζ-potential were reproducible to within ±4 mV of the mean value given by 16 determinations of ten data accumulations.

Transmission electron microscopy measurements

The c-Myc particles were fixed in 2.5% glutaraldehyde in 0.1 M sodium cacodylate buffer for 30 min on ice. After rinsing the pellet that was obtained post-centrifugation, the particles were sequentially stained with 1.25% osmium tetroxide, 2% tannic acid and uranyl acetate, following which the pellet was dehydrated and embedded in Poly/Bed® 812 (Polysciences, Inc., PA, USA). The pellet was then thin-sectioned on a Reichert–Jung Ultracut (Depew, NY, USA) and post-stained in uranyl acetate and lead citrate.

Results & discussion

Our strategy to prepare the Sn-2 PD involved relatively simple alterations of the index compound 10058-F4 [14] in order to introduce a short piperidine amine moiety for further functionalization through the amine end (Figure 2). c-Myc inhibitor-1 was synthesized in a straightforward way. Briefly, 4-ethyl benzaldehyde

underwent an aldol condensation reaction with rhodanine in the presence of a catalytic amount of Tween® 80 (Sigma Aldrich, Inc., MO, USA) in potassium carbonate solution at ambient temperature. The mixture was neutralized with 5% HCl and the precipitant was treated with saturated sodium hydrogen sulfite ($NaHSO_3$), then recrystallized with aqueous ethanol in order to produce bright yellow-colored compound in 72% yield. This rhodanine derivative was reacted to piperidine-mono-tert-boc (N-tert-butoxycarbonyl) and formaldehyde. Deprotection of the tert-boc in presence of 1:1 HCl in dioxane produced c-Myc inhibitor-1. Finally, c-Myc inhibitor-1 was esterified by 1-palmitoyl-2-azelaoyl PC (phosphocholine) (fatty acid-modified oxidized lipid 16:0–9:0 COOH PC)/dicyclohexyl carbidiimide/4-dimethyl amino pyridine-mediated coupling to produce c-Myc-rhodanine PD (c-Myc-PD) at a 43% yield. The structures of all of the small-molecule precursors and c-Myc inhibitors were characterized by ^{1}H-nuclear magnetic resonance and mass spectrometric analyses and matched well with published reports [14,15].

For the incorporation of the PDs, two strategies were followed (Figure 1). While the vascularly constrained NPs (<200 nm, PFC cored) are designed to limit extravasation into tissues in order to enhance the specificity of vascular targeting, such as to endothelial biomarkers of angiogenesis, the anticipated application also demanded a much smaller NP (<20 nm, polysorbate cored) for penetration from blood into the cancer cells. All particles are cleared by the monocyte phagocytic system, predominantly in the liver, spleen and marrow. Large particles, such as the PFC agents designed to recognize vascular epitopes, saturate their targets in 2–3 h and the elimination of unbound particles through clearance organs promotes the metabolism and elimination of the excess fraction. Stable smaller particles of <20 nm tend to have longer half-lives and better opportunity for extravascular access given adequate circulatory concentrations in order to maintain appropriate concentration gradients for passive dissemination. Our attempts to prepare any intermediate-sized NPs (~50 nm) were not successful. The feasibility of deriving such NPs was beyond the scope of our present study and further approaches might be necessary in the near future.

Briefly, the NPs were prepared as a microfluidized suspension of 20% (v/v; for bigger PFC NPs, perfluorooctylbromide was used [Exfluor, Inc.]; for smaller polysorbate NPs, sorbitan sesquileate was used [Sigma Aldrich, Inc., MO, USA]), 2.0% (w/v) of a surfactant comixture and 1.7% (w/v) glycerin in pH 6.5 carbonate buffer. An $\alpha_v\beta_3$-integrin antagonist (a quinolone nonpeptide) was used for homing

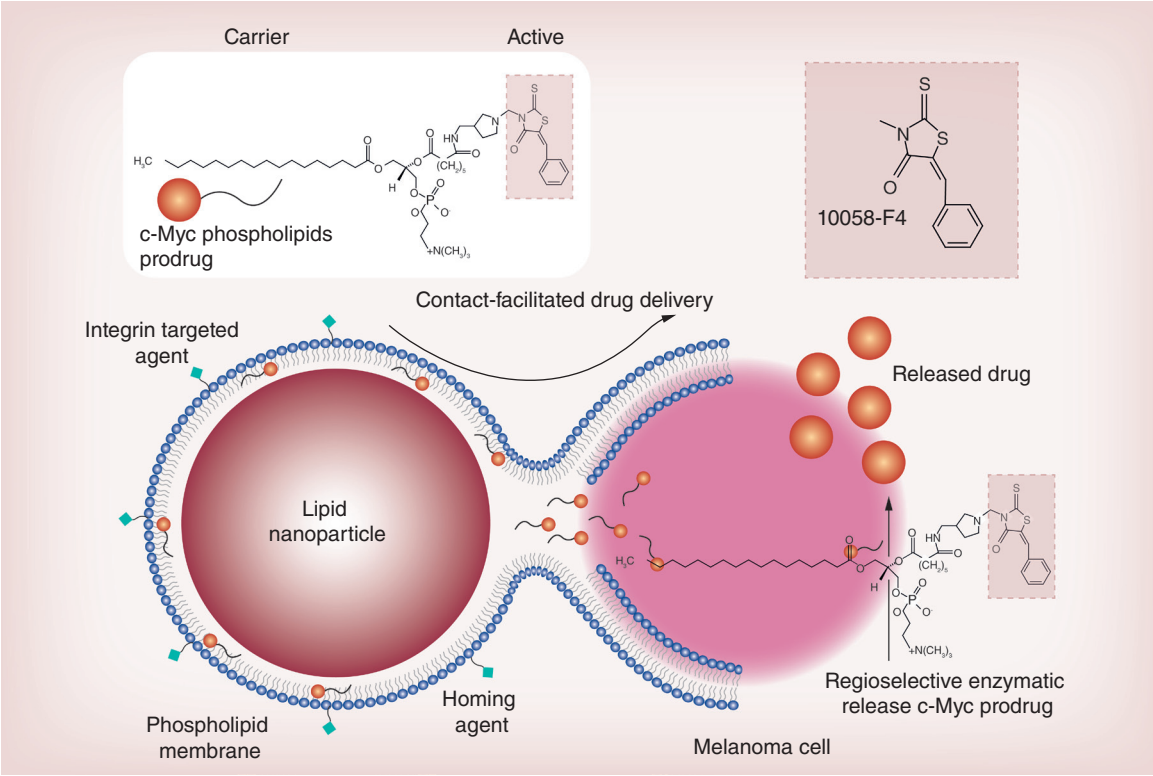

Figure 2. Combating melanoma: a graphical representation of the c-Myc inhibitor (10058-F4) delivery by a phospholipid-coated nanoparticle via the contact-facilitated drug delivery approach.

angiogenesis [18]. The surfactant comixture of NPs included 2 mol% (could be increased ≤10 mol%) of c-Myc-PD, 0.15 mol% of $\alpha_v\beta_3$-ligand-conjugated lipid and approximately 96.5 mol% (or 88.5 mol%) of lecithin. Nontargeted NPs excluded the homing ligands. The surfactant components for each formulation were combined with the PFC, buffer and glycerin, and the mixtures were homogenized at 20,000 psi for 4 min at 4°C. The NPs were preserved in sterile sealed vials until use.

Upon completion of the synthesis, NPs were thoroughly characterized by physicochemical techniques (e.g., dynamic light scattering, ζ-potential and transmission electron microscopy; Figure 1). Dynamic light scattering measurements revealed the nominal hydrodynamic diameters of the $\alpha_v\beta_3$-targeted c-Myc-PD and control samples in aqueous solution. Incorporation of the PD at 2–10 mol% within the surfactant comixture resulted in minimal changes in particle sizes (Figure 3). ζ-potential values of the NPs were negative (approximately -20 ± 6 mV), which confirms successful phospholipid encapsulation of the NPs and accounts for the overall stability. Hydrodynamic particle sizes for the c-Myc-PD-incorporated PFC NPs and polysorbate micelles were 210 ± 32 and 16 ± 4 nm, respectively, for the targeted nanoparticles with narrow distribution (polydispersity index: ~0.1–0.2). The presence of negative ζ-potential values for all of these particles points to their colloidal stability and successful phospholipid encapsulation. These particles were further analyzed by transmission electron microscopy in order to observe their morphologies in the anhydrous state. The particles were found to be spherical with distinct dark peripheries of lipid encapsulation (Figure 1G). The average particle diameter was calculated to be 172 ± 66 nm (measured from 141 particles) and 14 ± 6 nm for PFC

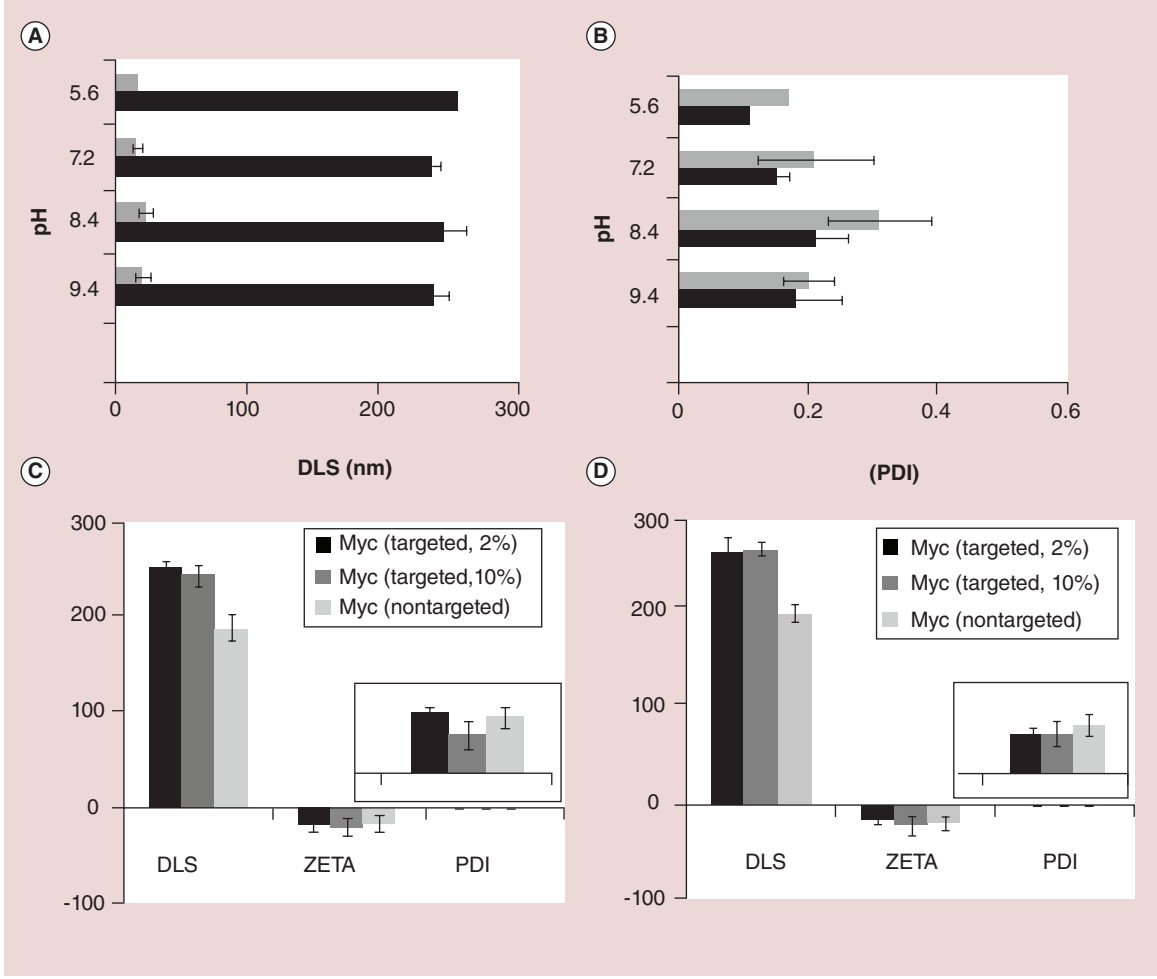

Figure 3. Stability and physico-chemical characterization results. pH stability of the targeted perfluorocarbon nanoparticles (black) and polysorbate nanoparticles (gray) within the physiological pH range 5.9–9.4 observed as changes in **(A)** DLS and **(B)** PDI measurements. Stability indexes are shown **(C)** immediately after preparation and **(D)** over 6 months for the targeted and nontargeted nanoparticles.

and polysorbate particles, respectively (Figure 1F & G). Atomic force microscopy (AFM) images of the polysorbate micelles confirmed that these particles were spherical in the anhydrous state (Figure 1H). Careful observation of the hydrodynamic size, ζ-potential and polydispersity index suggests that these particles possess long shelf-life stability and retain their particle integrity over a prolonged period of time (>5 months; Figure 3) and over varying pH values (Figure 3). The particles were found to retain their integrity over a physiological pH range of 5.6–9.4 (Figure 3). UV–visible spectroscopy confirmed the absorbences at 280–320 nm, corresponding to the presence of the conjugated thiazolidinone moiety as a part of the c-Myc inhibitor within the NPs. The drug was well retained with less than 5% of the incorporated dosage diffusing out from the NPs under infinite sink conditions during *in vitro* dissolution.

For *in vitro* evaluation, four targeted and control groups of NPs were prepared. These included: $\alpha_v\beta_3$-c-Myc-PD PFC NPs (2%); $\alpha_v\beta_3$-ND NPs; NT-c-Myc-PD PFC NPs (2%); and $\alpha_v\beta_3$-targeted polysorbate NPs (Figure 4). Upon completion of the synthesis and characterization of the PD and development of the $\alpha_v\beta_3$-targeted c-Myc-PD NPs and controls, the efficacies of the particles were evaluated *in vitro* in mouse (B16-F10) and human (C32) melanoma cell lines (Figure 4). After establishing the culture, cells were exposed to $\alpha_v\beta_3$-c-Myc-PD PFC NPs, NT-c-Myc-PD PFC NP, $\alpha_v\beta_3$-c-Myc-PD polysorbate NPs and $\alpha_v\beta_3$-ND NPs diluted 1:500 from the stock 20% emulsions (v/v; 100 µl). Mouse melanoma cells were additionally treated with equivalent volumes of free c-Myc inhibitor in DMSO (equimolar to the NP dose), DMSO and culture media (control). Unbound or unincorporated drugs were removed after 30 min by gentle serial washing, followed by replacement of the media and continued incubation.

To further assess the potential susceptibility of c-Myc-PD in NPs for premature lipase liberation, drug-encapsulated NPs (200 µl) were incubated with 3 ml of fresh plasma or fresh whole blood preserved with EDTA spiked with 200 µl 0.9% NaCl and 0.2 mg phospholipase A2. This was referenced to an equimolar amount of 12 mM $CaCl_2$ c-Myc (10058-F4) or cMyc-PD in DMSO diluted in 3 ml of phosphate-buffered saline at pH 7.4. The samples were continuously agitated on a nutator to prevent settling. As a positive control, 200 µl of isopropanol was added to the lipase-spiked plasma containing c-Myc-PD in NPs in order to 'crack' the particles' integrity, exposing the lipase-labile PD to the enzyme-rich plasma milieu. The plasma–enzyme–NP mixture (200 µl) was combined with 200 µl Cleanascite for lipid removal and clarification (Biotech Support Group, Inc., NJ, USA) at 25°C for 15 min. The mixture was centrifuged at 5000 rpm (30 min) and the supernatant (200 µl) was analyzed by high-performance liquid chromatography and mass spectrometry in order to confirm the presence or absence of the cleaved product (Figure 5A).

Viable cell proliferation was determined using the alamarBlue assay at 24, 48 and 72 h post-treatment. The fluorescence signal was read at an emission wavelength of 580 nm with a 590-nm excitation wavelength. As shown in Figure 4D, $\alpha_v\beta_3$-c-Myc-PD PFC NPs decreased melanoma proliferation at 24, 48 and 72 h more so than equimolar treatment with the free drug in DMSO ($p < 0.05$). Mouse melanoma proliferation over the study did not differ between the culture media only, free c-Myc inhibitor in DMSO, DMSO alone, NT-c-Myc-PD PFC NPs or the $\alpha_v\beta_3$-ND NP groups ($p > 0.05$). Cell proliferation between $\alpha_v\beta_3$-c-Myc-PD PFC NPs and NT-c-Myc-PD PFC NPs did not differ, suggesting that the PFC NPs (specific gravity: 2.0) settled on the cells during incubation, leading to the *de facto* targeting and contact-facilitated drug delivery of the c-Myc-PD.

Preliminary pharmacokinetics and organ distribution studies were conducted in a rat model. The non-targeted particles were labeled with a trace amount of gadolinium (1 mol% of Gd^{3+} diethylene triamine pentaacetic acid bisoleate) on the surface of the particles for analytical detection with inductive coupled plasmon resonance. The pharmacokinetic profile of NT-c-Myc-PD NPs show the expected trend of 62 ± 1 and 122 ± 1 min, respectively, for bigger (200 nm) and smaller NPs (20 nm; Figure 5A). The organ distributions of both the 200- and 20-nm NPs based on gadolinium estimation in the major organs by inductive coupled plasmon resonance at 2 h following intravenous injection of NPs (1 mg/ml) are shown in Figure 5C & D. The preliminiary distributive properties were conducted in rats (n = 3 for smaller particle and n = 5 for bigger particles) for these particles indicate expected clearance of these particles following the reticuloendothelium system (RES) route.

It is warranted to study the enzymatic mechanisms and rate controlling elements affording the release of the c-Myc into the cytosol from the membrane. It is well known that phospholipase A2 is able to catalyze the hydrolysis of the Sn-2 ester bond in a variety of phospholipids in order to liberate a free fatty acid and a lysophospholipid. The broad classifications of these enzymes includes: secreted low-molecular-weight phospholipases; larger cytosolic calcium-dependent phospholipases; Ca^{2+}-independent phospholipases; platelet-activating factor acetylhydrolases; and lyso-

somal phospholipases [19]. The preliminary step of this mechanism is the hydrolysis of the Sn-2 ester bond followed by the conversion of liberated arachadonic acid into eicosanoids, which exert a wide range of physiological and pathological effects. Multiple family members of different types of phospholipases are present in endothelial cells. These enzymes present an array of potential activating agents within target cells. In addition to these lipases, further enzymes (e.g., serine hydrolases or other hydrolases) are present, which could liberate the PDs in order to release the active pharmaceutical ingredients into target cells.

We have very recently reported the concept of Sn-2 phospholipid PDs and demonstrated the utility of the system with fumagillin and taxane-based drugs [20]. Relevant reports of lipid-based PDs were considered previously for two compounds – indomethacin and valproic acid [21,22] – in order to enable oral controlled release of drugs by continuous degradation of the phospholipid PDs within the intestine. Unfortu-

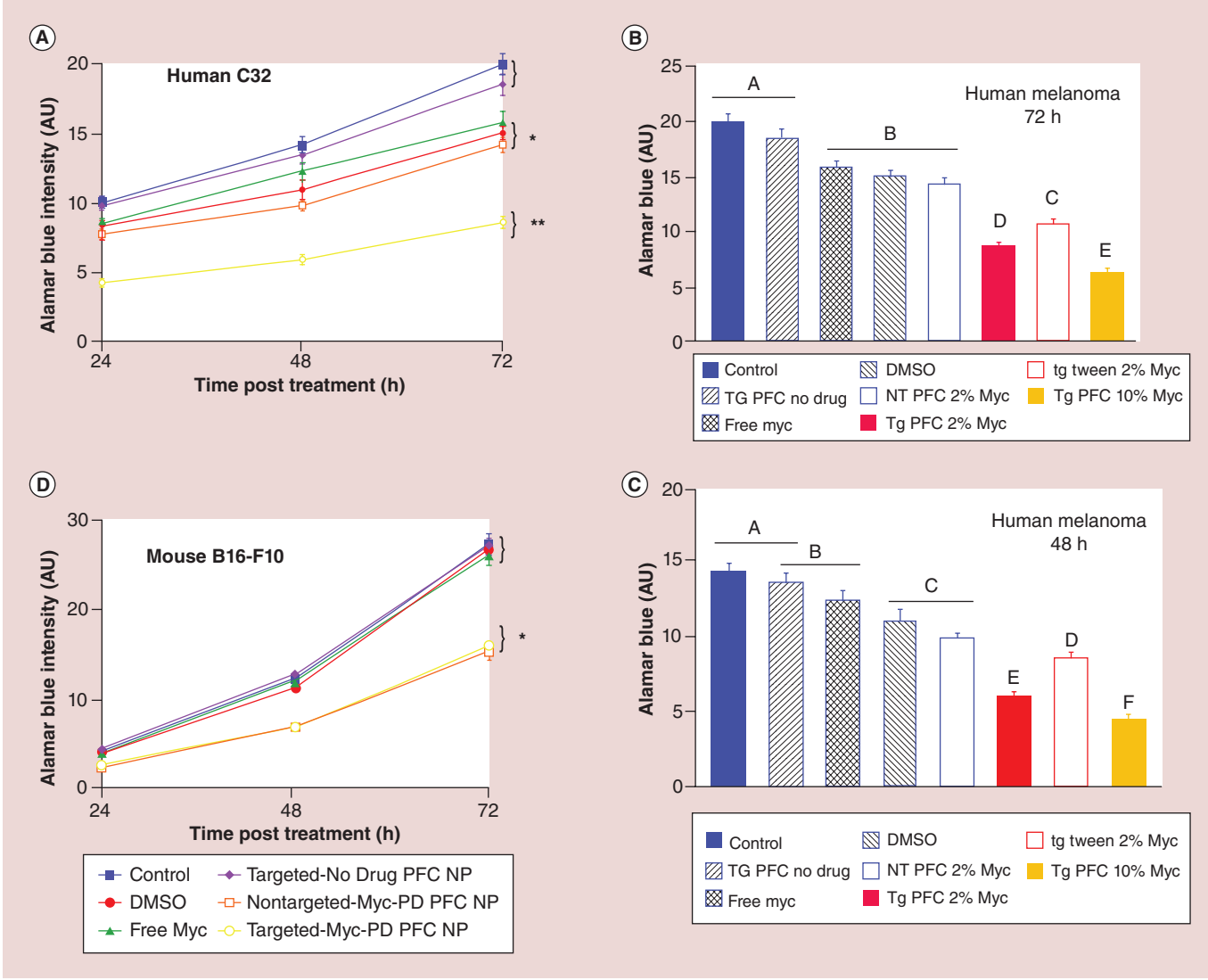

Figure 4. *In vitro* cell viability of c-Myc prodrug nanoparticles and controls. AlamarBlue® assay (Invitrogen, CA, USA) in **(A–C)** human melanoma C32 cells at 24, 48 and 72 h and **(D)** in mouse melanoma B16-F10 cells. A replicate cell culture experiment was conducted in order to corroborate the mouse response for human melanoma (C32; **A–C**). After 24h of incubation as described above, the cells were treated for 30 min with $\alpha_v\beta_3$-targeted c-Myc prodrug perfluorocarbon nanoparticles, $\alpha_v\beta_3$-targeted c-Myc prodrug polysorbate nanoparticles, nontargeted c-Myc prodrug perfluorocarbon nanoparticles, $\alpha_v\beta_3$-targeted no drug perfluorocarbon nanoparticles, free c-Myc inhibitor in DMSO, DMSO or culture media (control) as described above. Viable cell proliferation was determined using the AlamarBlue assay at 24, 48 and 72 h post-treatment. Human melanoma proliferation response over the 72-h study showed that both $\alpha_v\beta_3$-targeted c-Myc prodrug perfluorocarbon nanoparticles and $\alpha_v\beta_3$-targeted c-Myc prodrug polysorbate nanoparticles decreased melanoma proliferation at 24, 48 and 72 h more so than equimolar free c-Myc inhibitor ($p < 0.05$) or any other treatment.
AU: Arbitrary unit; NP: Nanoparticle; NT: No treatment; PD: Prodrug; PFC: Perfluorocarbon; TG: Targeted nanoparticle.

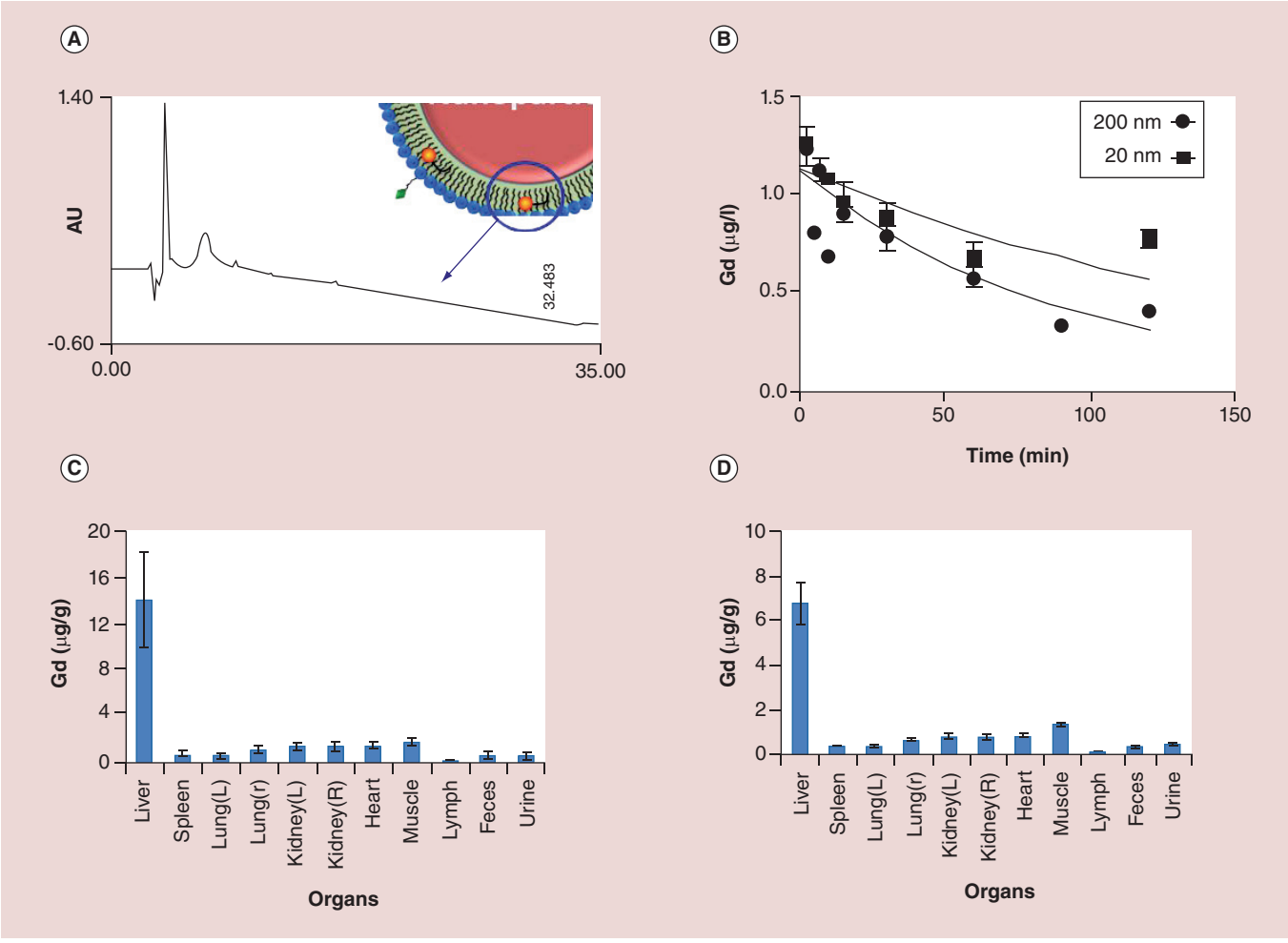

Figure 5. Stability of the lipid prodrugs and *in vivo* pharmacokinetics, biodistribution and clearance of c-Myc prodrug-loaded nanoparticles in rats. **(A)** representative high-performance liquid chromatography trace of c-Myc prodrug-loaded nanoparticles (200 nm) showing the absence of signature lipid–prodrug profile prior to disruption of the membrane. The blue arrow indicates absence of cMyc signature peak. **(B)** Pharmacokinetic profile of nontargeted c-Myc prodrug-loaded nanoparticles showing the expected trend. **(C & D)** Organ distribution of both **(C)** 200 nm and **(D)** 20 nm nanoparticles based on the Gd estimation of the major organs by inductive coupled plasmon resonance at 2 h following intravenous injection of the nanoparticles (1 mg/ml). Bars/data points and error bars in **(B–D)** represent mean ± standard deviation.
AU: Arbitrary unit; Gd: Gadolinium; L: Left; R: Right.

nately, the conceptual approach failed since the oral administration of an indomethacin PD lowered the bioavailability of the drug in comparison with the administration of free indomethacin [23]. When these PDs were administered intravenously as an untargeted liposome, the bioavailability of the PD was further reduced relative to oral administration of the phospholipid PDs and free drug. While using a nontargeted liposomal delivery approach or introducing a short spacer between the active pharmaceutical ingredient and Sn-2 ester improves the bioavailability, the effectiveness was only slightly greater [22–27]. We have recently shown that the accessibility and release of the active compound by circulating lipases was negligible for docetaxel PDs in lipid particles [28]. Similarly, the exchange of the PD from the particles to circulating erythrocytes was not detectable. As illustrated *in vitro* in this report and *in vivo* in others, these PDs require targeted binding and membrane hemifusion for effective therapy.

Conclusion

In conclusion, we report for the first time the therapeutic targeting of oncogenic c-Myc in human and mouse melanoma using an efficient, commercially amenable synthesis of c-Myc-PDs stably incorporated into lipid-encapsulated NPs. Lipid NPs differing greatly in size, composition and morphology were synthesized and characterized in order to illustrate the versatility of the PD concept. The novel c-Myc-PD was effectively

delivered with greater potency than the free compound with $\alpha_v\beta_3$-targeted NPs via the contact-facilitated drug delivery mechanism. We suggest that targeted c-Myc-PD NPs may provide a clinically viable systemic approach to c-Myc–Max antagonism. Studies assessing the applicability of the present system for *in vivo* targeted drug delivery are presently underway in our laboratories.

Future perspective

We report a novel synthetic strategy for Sn-2 lipase-cleavable c-Myc–Max antagonist PDs in combination with integrin-targeted nanotherapy for melanoma. We demonstrated that both intravascular (~200 nm) and extravascular (~20 nm) c-Myc NPs markedly decreased human and mouse cell proliferation more effectively than the free drug at equimolar concentrations. With these promising findings, further in-depth *in vivo* targeting studies are warranted in order to understand the translational potential of the system.

Financial & competing interests disclosure

The financial support from the American Heart Association (AHA) (0835426N and 11IRG5690011), NIH (under the grants NS059302, CA119342, CA1547371, NS073457 and HL073646) and the National Cancer Institute (NCI; under the grant N01CO37007) is greatly appreciated. The authors have no other relevant affiliations or financial involvement with any organization or entity with a financial interest in or financial conflict with the subject matter or materials discussed in the manuscript apart from those disclosed.

No writing assistance was utilized in the production of this manuscript.

Ethical conduct of research

The authors state that they have obtained appropriate institutional review board approval or have followed the principles outlined in the Declaration of Helsinki for all human or animal experimental investigations. In addition, for investigations involving human subjects, informed consent has been obtained from the participants involved.

Executive summary

- We developed a novel strategy for delivering oncogenic c-Myc inhibitors for targeting melanoma cells.
- c-Myc prodrugs (PDs) were developed based on Sn-2 phospholipid PDs by coupling 10058-F4, a known small molecule for disrupting c-Myc–Max inhibition, through the Sn-2 acyl position of an oxidized lipid.
- PDs were formulated in tiny polysorbate particles (20 nm) and perfluorocarbon nanoparticles (~200 nm).
- The efficacies of $\alpha_v\beta_3$-targeted and nontargeted c-Myc nanoparticles were studied in human C32 and mouse B16-F10 cells.
- The c-Myc-PD provided superior inhibition of proliferation and viability versus the native drug when targeted to melanoma cells *in vitro*.
- This unique approach improved circulatory retention of c-Myc-PDs and, in combination with lipid-based nanoparticles, may facilitate the translation of oncogenic c-Myc inhibitors.

References

Papers of special note have been highlighted as: • of interest

1 Gearhart J, Pashos EE, Prasad MK. Pluripotency redux – advances in stem-cell research. *N. Engl. J. Med.* 357, 1469–1472 (2007).

2 Lüscher B. Function and regulation of the transcription factors of the Myc/Max/Mad network. *Gene* 277, 1–14 (2001).

3 Cotterman R, Jin VX, Krig SR *et al.* N-Myc regulates a widespread euchromatic program in the human genome partially independent of its role as a classical transcription factor. *Cancer Res.* 68(23), 9654–9662 (2008).

4 Schlagbauer-Wadl H, Griffioen M, van Elsas A *et al.* Influence of increased c-Myc expression on the growth characteristics of human melanoma. *J. Invest. Dermatol.* 112(3), 332–336 (1999).

5 Kraehn GM, Utikal J, Udart M *et al.* Extra *c-myc* oncogene copies in high risk cutaneous malignant melanoma and melanoma metastases. *Br. J. Cancer* 84(1), 72–79 (2001).

6 Chana JS, Grover R, Wilson GD *et al.* The prognostic importance of *c-myc* oncogene expression in head and neck melanoma. *Ann. Plast. Surg.* 47(2), 172–177 (2001).

7 Nair SK, Burley SK. X-ray structures of Myc–Max and Mad–Max recognizing DNA. Molecular bases of regulation by proto-oncogenic transcription factors. *Cell* 112(2), 193–205 (2003).

8 D'Agnano I, Valentini IA, Fornari C *et al.* Myc down-regulation induces apoptosis in M14 melanoma cells by increasing p27(kip1) levels. *Oncogene* 20(22), 2814–2825 (2001).

9 Chen Z, Zeng H, Guo Y *et al.* miRNA-145 inhibits non-small cell lung cancer cell proliferation by targeting c-Myc. *J. Exp. Clin. Cancer Res.* 29, 151 (2010).

10 Soucek L, Jucker RL, Panacchia R, Ricordy F, Tatò SN. Omomyc, a potential Myc dominant negative, enhances Myc-induced apoptosis. *Cancer Res.* 62(12), 3507–3510 (2002).

11 Berg T, Cohen SB, Desharnais J *et al.* Small-molecule antagonists of Myc/Max dimerization inhibit Myc-induced transformation of chicken embryo fibroblasts. *Proc. Natl Acad. Sci. USA* 99(6), 3830–3835 (2002).

12 Yin X, Giap C, Lazo JS, Prochownik EV. Low molecular weight inhibitors of Myc–Max interaction and function. *Oncogene* 22(40), 6151–6159 (2003).

13 Mustata G, Follis AV, Hammoudeh DI *et al.* Discovery of novel Myc–Max heterodimer disruptors with a three-dimensional pharmacophore model. *J. Med. Chem.* 52(5), 1247–1250 (2009).

14 Prochownik EV, Giap C, Lazo JS, Yin X. US7026343: Improved low molecular weight myc–max inhibitors. (2006).

15 Wang H, Hammoudeh DI, Follis AV *et al.* Improved low molecular weight Myc–Max inhibitors. *Mol. Cancer Ther.* 6(9), 2399–2408 (2007).

16 Lin CP, Liu JD, Chow JM, Liu, CR, Liu HE. Small-molecule c-Myc inhibitor, 10058-F4, inhibits proliferation, downregulates human telomerase reverse transcriptase and enhances chemosensitivity in human hepatocellular carcinoma cells. *Anticancer Drugs* 18(2), 161–170 (2007).

17 Caruthers SD, Cyrus T, Winter PM, Wickline SA, Lanza GM. Anti-angiogenic perfluorocarbon nanoparticles for diagnosis and treatment of atherosclerosis. *Wiley Interdiscip. Rev. Nanomed. Nanobiotechnol.* 1(3), 311–323 (2009).

18 Pan D, Sanyal N, Schmieder AH *et al.* Antiangiogenic nanotherapy with lipase-labile Sn-2 fumagillin prodrug. *Nanomedicine* 7(10), 1507–1519 (2012).

- **Example of the formation of fumagillin Sn-2 phospholipid prodrugs for antiangiogenic nanotherapy.**

19 Burke J, Dennis E. Phospholipase A2 biochemistry. phospholipase A2 biochemistry. *Cardiovasc. Drugs Ther.* 23, 49–59 (2009).

20 Zhou HF, Yan H, Senpan A *et al.* Suppression of inflammation in a mouse model of rheumatoid arthritis using targeted lipase-labile fumagillin prodrug nanoparticles. *Biomaterials* 33(33), 8632–8640 (2012).

21 Arik D, Duvdevani R, Shapiro I, Elmann A, Finkelstein E, Hoffman A. The oral absorption of phospholipid prodrugs: *in vivo* and *in vitro* mechanistic investigation of trafficking of a lecithin-valproic acid conjugate following oral administration. *J. Control. Release* 126, 1–9 (2008).

22 Dahan A, Duvdevani R, Dvir E, Elmann A, Hoffman A. A novel mechanism for oral controlled release of drugs by continuous degradation of a phospholipid prodrug along the intestine: *in-vivo* and *in-vitro* evaluation of an indomethacin–lecithin conjugate. *J. Control. Release* 119, 86–93 (2007).

- **Earlier examples of the formation of Sn-2 phospholipid prodrugs of indomethacin and valproic acid.**

23 Davidsen J, Jørgensen K, Andresen TL, Mouritsen OG. Secreted phospholipase A2 as a new enzymatic trigger mechanism for localised liposomal drug release and absorption in diseased tissue. *Biochim. Biophys. Acta* 1609(1), 95–101 (2003).

24 Andresen TL, Davidsen J, Begtrup M, Mouritsen OG, Jørgensen K. Enzymatic release of antitumor ether lipids by specific phospholipase A2 activation of liposome forming prodrugs. *J. Med. Chem.* 47(7), 1694–1703 (2004).

25 Jensen SS, Andresen TL, Davidsen J *et al.* Secretory phospholipase A2 as tumor-specific trigger for targeted delivery of a novel class of liposomal prodrug anticancer ether lipids. *Mol. Cancer Ther.* 3(11), 1451–1458 (2004).

26 Andresen TL, Jensen SS, Kaasgaard T, Jørgensen K. Triggered activation and release of liposomal prodrugs and drugs in cancer tissue by secretory phospholipase A2. *Curr. Drug Deliv.* 2(4), 353–362 (2005).

27 Peters G, Møller M, Jørgensen K, Rönnholm P, Mikkelsen M, Andresen T. Secretory phospholipase A2 hydrolysis of phospholipid analogues is dependent on water accessibility to the active site. *J. Am. Chem. Soc.* 129(17), 5451–5461 (2007).

28 Pan D, Schmieder AH, Wang K *et al.* Anti-angiogenesis therapy in the Vx2 rabbit cancer model with a lipase-cleavable Sn 2 taxane phospholipid prodrug using α(v) β?-targeted theranostic nanoparticles.. *Theranostics.* 4(6), 565–578 (2014).